mathematics

MDPI

Article

Impact of the Allee Effect on the Dynamics of a Predator–Prey Model Exhibiting Group Defense

Manoj Kumar Singh [1], Arushi Sharma [1] and Luis M. Sánchez-Ruiz [2,*]

[1] Department of Mathematics and Statistics, Banasthali Vidyapith, Tonk 304022, India; s.manojbbau@gmail.com (M.K.S.); arushi.kannav@gmail.com (A.S.)
[2] Departamento de Matemática Aplicada, Universitat Politècnica de València, 46022 Valencia, Spain
* Correspondence: lmsr@mat.upv.es

Abstract: The Allee effect and group defense are two naturally occurring phenomena in the prey species of a predator–prey system. This research paper examines the impact of integrating the Allee effect on the dynamics of a predator–prey model, including a density-dependent functional response that reflects the defensive strategies of the prey population. Initially, the positivity and boundedness of the solutions are examined to ascertain the biological validity of the model. The presence of ecologically significant equilibrium points are established, followed by examining parametric restrictions for the local stability to comprehend the system dynamics in response to minor perturbations. A detailed computation encompasses diverse bifurcations, both of codimension one and two, which provide distinct dynamic behaviors of the model, such as oscillations, stable coexistence, and potential extinction scenarios. Numerical simulation has been provided to showcase complex dynamical behavior resulting from the Allee effect and prey group defense.

Keywords: predator–prey model; stability; bifurcation; multiplicative Allee effect; group defense

MSC: 92D25; 34C23; 34K60



Academic Editor: Huaizhong Zhao

Received: 15 January 2025
Revised: 6 February 2025
Accepted: 12 February 2025
Published: 14 February 2025

Citation: Singh, M.K.; Sharma, A.; Sánchez-Ruiz, L.M. Impact of the Allee Effect on the Dynamics of a Predator–Prey Model Exhibiting Group Defense. *Mathematics* **2025**, *13*, 633. https://doi.org/10.3390/math13040633

Copyright: © 2025 by the authors. Licensee MDPI, Basel, Switzerland. This article is an open access article distributed under the terms and conditions of the Creative Commons Attribution (CC BY) license (https://creativecommons.org/licenses/by/4.0/).

1. Introduction

Predator–prey interactions are intricate, foundational, and complex components of our ecosystem, influencing population dynamics and species coexistence, triggering trophic cascades, etc. Preserving and understanding these interactions for the stability of the ecosystem, its resilience, and maintaining the overall health of the planet are essential. The traditional predator–prey model coined by Lotka [1] and Volterra [2] assumes simple dynamics. However, real-world predator–prey interactions exhibit complex phenomena that require more nuanced approaches, and two such phenomena are the Allee effect [3–5] and group defense [6–8]. In this research work, we conceptualize and then analyze a model that demonstrates predator–prey interaction along with the integration of group defense and the multiplicative Allee effect in prey, both of which significantly influence population dynamics.

The behavioral strategy of prey in which the prey species collaboratively reduces predation risk is termed group defense. This phenomenon enhances individual survival through mechanisms like improved vigilance, coordinated defense, etc. The incorporation of group defense into predator–prey models provides insight into how social behaviors

shape population stability and ecological interactions. A predator–prey model used to demonstrate the phenomenon of group defense is given in [9]

$$\begin{aligned} \frac{dN}{dt} &= N(t)A(N,K) - P(t)f(N), \\ \frac{dP}{dt} &= P(t)(C(N) - D). \end{aligned} \tag{1}$$

Here, $N(t)$ and $P(t)$ give the density of the prey and predator populations, respectively. $A(N,K)$ represents the growth rate of the prey, $f(N)$ represents the response function, and $C(N)$ represents the prey to predator conversion. K and D indicate the carrying capacity and the predator's death rate, respectively. The assumption for the response function, say $f(N)$, used to model group defense is given in [10]

$$f(0) = 0,\ f(N) > 0 \text{ for } N > 0, \tag{2}$$

and $M > 0$ such that

$$f'(N) > 0 \text{ for } 0 \leq N < M, \tag{3}$$

and

$$f'(N) < 0 \text{ for } N > M. \tag{4}$$

Freedman and Ruan [11] devised a non-monotonic functional response $f(N) = \alpha N e^{-\beta N}$, where α and β are positive constants, to capture the dynamics of group defense behavior as it satisfies the conditions given in (2)–(4). Rothe and Shafer [12] used the so-called Holling type IV functional response $f(N) = \frac{N}{a+bN+N^2}$, satisfying conditions (2)–(4), to represent group defense. Figure 1 depicts that though both curves reach the same height, even with the same rate at their peak, the decline rate of the Freedman and Ruan (F-R) function is comparatively sharper than Holling type IV, so in this study we have used the F-R function to represent group defense (ref. Figure 1). In addition, the impact of α and β on the shape of the curve of the functional response $f(N) = \alpha N e^{-\beta N}$ is depicted in Figure 2. It can be observed that as α increases, the convexity of the curve increases, while as β increases, the convexity of the curve decreases, implying positive and negative correlations of the constants with the functional response, respectively.

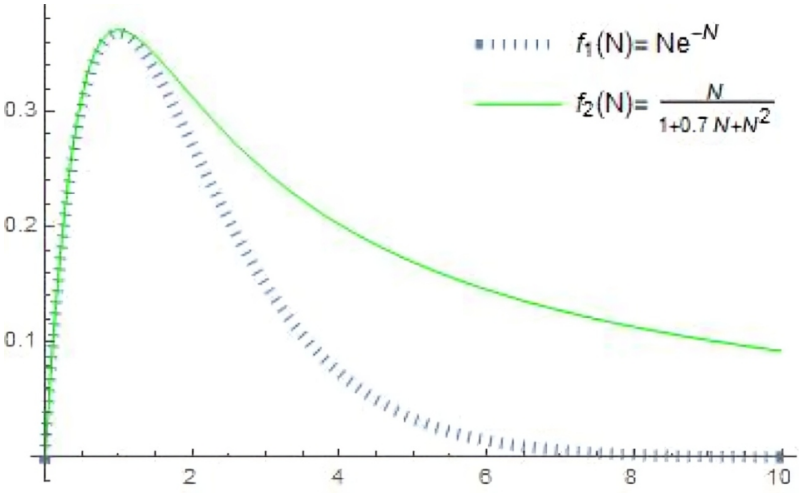
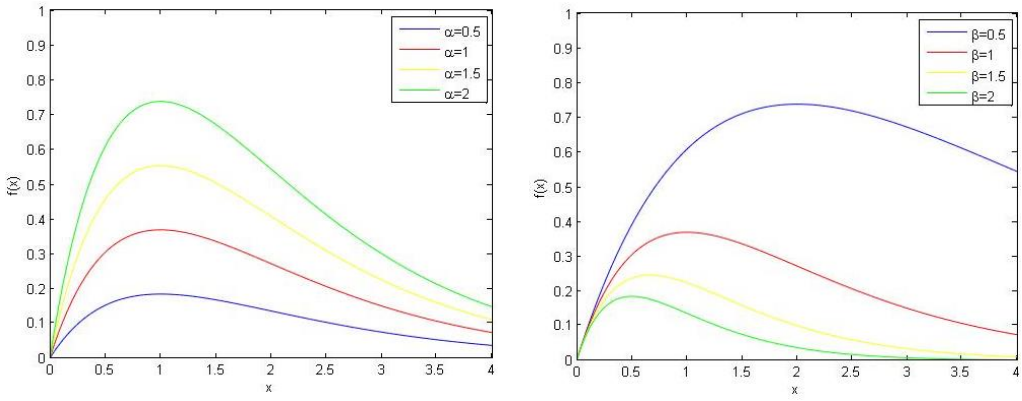


Figure 1. A Freedman and Ruan function (blue dotted curve) $f_1(N) = Ne^{-N}$ and a Holling type IV function (green curve) $f_2(N) = \frac{N}{1 + 0.7N + N^2}$.



(**a**) (**b**)

Figure 2. Variation in functional response $f(x) = \alpha x e^{-\beta x}$ with α and β: (**a**) As α increases, the convexity of the curve increases. (**b**) As β increases, the convexity of the curve decreases.

Sasmal and Takeuchi [13] studied how a predator–prey system behaves under the influence of group defense and fear. Jiao et al. [6] explored the Filippov Leslie–Gower predator–prey (LGPP) model that exhibits the phenomenon of group defense in the presence of delay. Das et al. [14] studied a diseased predator–prey model in which harvesting is carried out and the prey presents group defense strategies. Pratama et al. [15] assessed how group defense and fear affect predator–prey systems with the Holling type IV functional response and experiencing intraspecific competition. Pal et al. [16] evaluated a predator–prey system that focuses on the impact of fear induced in prey due to the presence of predators and where prey adopts group defense mechanisms. Singh and Sharma [8] explored how harvesting and group defense influence the dynamics of a predator–prey model. Numerous studies have also examined the dynamics of group defense in different ecological models [17–21].

Ecologist W.C. Allee devised the Allee effect, which indicates a positive correlation between population density and individual fitness, which can occur due to a decrease in cooperative behaviors such as mating, herding, and parental care within the species. This phenomenon is widely studied due to its essential role in determining whether a species survives or goes extinct. The multiplicative Allee effect combines density-dependent survival and reproduction, amplifying its impact on population dynamics. Various researchers have explored the Allee effect coupled with a few other phenomena. Rahmi et al. [22] analyzed the memory effect, along with the incorporation of the double Allee effect in the predator population, in a modified LGPP model. They analyzed both strong and weak Allee effects. Yin et al. [23] explored the Allee effect on the system dynamics of an LGPP model that incorporates the presence of prey refuge. Cruz [24] demonstrated the impact of delay on the stability of the LGPP model in the presence of a strong Allee effect. Sen et al. [25] conducted a bifurcation analysis of the complex dynamics of the predator–prey model with the Allee effect in the predator. Shang and Qiao [26] focused on the study of the double Allee effect in the modified Holling and LGPP model, which is being harvested. Singh et al. [27] analyzed the LGPP model, integrating the phenomena of the double Allee effect and the fear effect.

Even though the phenomena of the Allee effect and group defense have been widely studied in predator–prey interactions individually, the impact of both these phenomena occurring simultaneously remains under-explored. This work offers significant insights into the influence of the initial conditions, group defense, and Allee effect parameters on the stability and behavior of the proposed model. This study comprises seven sections. The conceptualization of the model under study, where group defense the and multiplicative Allee effect are introduced in the system, is presented in Section 2. The well-posedness of

the proposed system is also included. Subsequently, Section 3 includes the reckoning of the equilibrium points with the analysis of their stability. In Section 4, bifurcation analysis is included. The emergence of saddle-node, Hopf, and Bogadanov–Takens bifurcation has been discussed in great detail along with the numerical simulation and phase portraits. After this, Section 5 sheds light on the impact of the introduced parameters, both analytically and graphically. Section 6 concludes the entire work by providing an in-depth review of the established results while performing an analysis.

2. Conceptualization of the Model

2.1. Base Model

Xiao and Ruan [28], in their study, considered that the growth rate of the prey $A(N, K)$ is governed by the logistic growth function; the predator response function is taken as $P(N) = \alpha e^{-\eta N}$, where α and η are positive constants, and the prey to predator conversion rate $C(N)$ showcases similar properties as $P(N)$ and is taken as $C(N) = \mu P(N)$. So, System (1) comes out to be

$$\begin{aligned} \frac{dN}{dT} &= rN\left(1 - \frac{N}{K}\right) - \alpha NPe^{-\eta N}, \\ \frac{dP}{dT} &= P\left(\mu\alpha Ne^{-\eta N} - D\right), \end{aligned} \tag{5}$$

where $N \equiv N(T)$ and $P \equiv P(T)$ denote the prey and predator densities at time T, respectively. Here, $r > 0$ denotes the intrinsic growth rate of the prey, $K > 0$ denotes the carrying capacity, and $D > 0$ denotes the predator's death rate. Also, α and η are positive.

2.2. Modified Model

Integrating the multiplicative Allee effect (ref. González-Olivares et al. [29]) in System (5), we obtain

$$\begin{aligned} \frac{dN}{dT} &= rN\left(1 - \frac{N}{K}\right)(N - M) - \alpha NPe^{-\eta N}, \\ \frac{dP}{dT} &= P\left(\mu\alpha Ne^{-\eta N} - D\right), \end{aligned} \tag{6}$$

where $-K \leq M \leq K$ represents the Allee threshold. If $M > 0$, then the Allee effect is considered strong, while if $M \leq 0$, then it is considered weak [29]. In this work, we will analyze the presence of a strong Allee effect.

2.3. Simplification of the Model

To reduce the number of parameters, consider $N = Kx$, $P = \frac{ry}{\alpha}$, $t = rT$. Model (6) reduces to

$$\begin{aligned} \frac{dx}{dt} &= Kx(1 - x)(x - m) - xye^{-\beta x}, \\ \frac{dy}{dt} &= y(bxe^{-\beta x} - d), \end{aligned} \tag{7}$$

where $m = \frac{M}{K}$, $\beta = \eta K$, $b = \frac{\alpha uK}{r}$, $d = \frac{D}{r}$. From the standpoint of ecology, our analysis is centered on the dynamics of System (7) in the closure $\overline{R^2_+}$ of the first quadrant R^2_+. Consequently, we focus on ecologically relevant initial conditions $x(0) \geq 0$, $y(0) \geq 0$.

System (7) represents an ecological interaction of two species, so every solution of this system must be ecologically relevant.

Lemma 1. *a. Every solution of System (7) starting in R^2_+ is positive for all future times.*
b. Every solution of System (7) starting in R^2_+ is bounded for all future times.

Proof. a. The equations in System (7) are integrated under the initial conditions $x(0) \geq 0,\ y(0) \geq 0$. The solution can be conveyed as

$$x(t) = x(0)exp\Big[\int_0^t (K(1-x(s))(x(s)-m) - y(s)e^{-\beta x(s)})\, ds\Big] > 0, \tag{8}$$

$$y(t) = y(0)exp\Big[\int_0^t y(s)\Big(bx(s)e^{-\beta x(s)} - d\Big)\, ds\Big] > 0. \tag{9}$$

Thus, the conclusion can be drawn that any solution which starts in R_+^2 remains in it for $t \geq 0$. Furthermore, for all future times, any solution trajectory that starts on the positive x-axis (or y-axis) will stay on that axis. Hence, the set R_+^2 is an invariant set.

b. Let $\phi = bx + y$. Now, we differentiate ϕ with respect to time; we obtain

$$\begin{aligned}\frac{d\phi}{dt} &= bKx(1-x)(x-m) - d\,y \\ &\leq bKx(\frac{(1+m)^2}{4} + \frac{d}{K}) - d\,\phi.\end{aligned}$$

Let, $\mu = max_{t\geq 0}\ bKx\Big(\frac{(1+m)^2}{4} + \frac{d}{K}\Big)$, which gives

$$\frac{d\phi}{dt} \leq \mu - d\,\phi.$$

Now, using Gronwall's inequality, we obtain

$$0 \leq \phi(x,y) \leq \frac{\mu}{d}\Big(1 - e^{-d\,t}\Big) + \phi(x(0),y(0))e^{-d\,t}$$

and as $t \to \infty$, we obtain $0 \leq \phi(x,y) \leq \frac{\mu}{d}$, which proves boundedness.

□

3. Dynamics of the Model

The feasible equilibrium points of System (7) are the non-negative solutions of the system

$$\begin{aligned}Kx(1-x)(x-m) - xye^{-\beta x} &= 0, \\ y(bxe^{-\beta x} - d) &= 0.\end{aligned} \tag{10}$$

Apart from the trivial solution, $E_0(0,0)$, System (10) has the following two types of solutions holding ecological importance:

(i) Predator-free equilibrium points: The abscissa of the predator-free solutions are obtained by the roots of the following equation

$$K(1-x)(x-m) = 0. \tag{11}$$

(ii) Coexistence equilibrium points: The abscissa of the coexistence equilibria of the System (7) are the positive solutions of the equation

$$bxe^{-\beta x} - d = 0. \tag{12}$$

The ordinates of feasible interior equilibrium points are $y = K(1-x)(x-m)e^{\beta x}$, provided $m < x < 1$.

Equation (12) has no solution whenever $b < e\beta d$ holds and has one positive root $x^* = \frac{1}{\beta}$ whenever $b = e\beta d$ holds. Moreover, Equation (12) has two non-negative roots x_1^* and x_2^* whenever $b > e\beta d$ holds [28]. The preceding discussion is encapsulated in the theorem below.

Theorem 1. *a. System (7) consistently exhibits three axial equilibrium points $E_0 = (0,0)$, $E_1 = (1,0)$ and $E_2 = (m,0)$.*

b. System (7) exhibits two interior equilibrium points $E_1^* = (x_1^*, y_1^*)$ and $E_2^* = (x_2^*, y_2^*)$ when $b > e\beta d$, one interior equilibrium point $E^* = (x^*, y^*)$ when $b = e\beta d$, and no interior equilibrium points when $b < e\beta d$.

Stability analysis:

To study the local stability of equilibrium points that System (7) exhibits, we find the Jacobian matrix at any point $E(x,y)$

$$J_E = \begin{bmatrix} Kx(1+m-2x) + K(1-x)(x-m) - ye^{-\beta x}(1-\beta x) & -xe^{-\beta x} \\ bye^{-\beta x}(1-\beta x) & bxe^{-\beta x} - d \end{bmatrix}.$$

Theorem 2. *The properties of axial equilibrium points are as follows:*

a. $E_0 = (0,0)$ is always an asymptotically stable point.

b. $E_1 = (1,0)$ is an asymptotically stable point if $be^{-\beta} < d$ and saddle point if $be^{-\beta} > d$.

c. $E_2 = (m,0)$ is an unstable point if $bme^{-m\beta} < d$ and saddle point if $bme^{-m\beta} > d$.

Proof. a. The eigenvalues of the Jacobian matrix J_{E_0} are $-mK$ and $-d$, which clearly indicates that $E_0 = (0,0)$ is an asymptotically stable point.

b. The eigenvalues of the Jacobian matrix J_{E_1} are $-K(1-m)$ and $be^{-\beta} - d$, which clearly indicates that $E_1 = (1,0)$ is a stable point if $be^{-\beta} < d$ and saddle point if $be^{-\beta} > d$.

c. The eigenvalues of the Jacobian matrix J_{E_1} are $Km(1-m)$ and $bme^{-m\beta} - d$, which clearly indicates that $E_2 = (m,0)$ is an unstable point if $bme^{-m\beta} < d$ and saddle point if $bme^{-m\beta} > d$.

□

Theorem 3. *a. The equilibrium point $E_1^* = (x_1^*, y_1^*)$ exists whenever $b > e\beta d$ holds and it is an asymptotically stable point when $K + mK + \beta y_1^* e^{-\beta x_1^*} < 2Kx_1^*$ and unstable point when $K + mK + \beta y_1^* e^{-\beta x_1^*} > 2Kx_1^*$.*

b. The equilibrium point $E_2^* = (x_2^*, y_2^*)$ exists whenever $b > e\beta d$ holds and it invariably constitutes a saddle point.

c. The equilibrium point $E^* = (x^*, y^*)$ exists whenever $b = e\beta d$ holds and it constitutes a degenerate singularity.

Proof. At the interior equilibrium point, say $E(x,y)$, the determinant and trace of the Jacobian matrix are

$$Det(J_E) = b\beta xe^{-\beta x}(\frac{1}{\beta} - x)K(1-x)(x-m)$$

and

$$Tr(J_E) = Kx(1+m+\beta x(1-x)(x-m) - 2x).$$

Clearly, $Det(J_{E^*}) = 0$, $Det(J_{E_1^*}) > 0$ and $Det(J_{E_2^*}) < 0$. Therefore, E^* is a degenerate singularity and E_2^* is always a saddle point. As $Tr(J_{E_1^*}) < 0$ when $K + mK + \beta y_1^* e^{-\beta x_1^*} < 2Kx_1^*$, and $Tr(J_{E_1^*}) > 0$ when $K + mK + \beta y_1^* e^{-\beta x_1^*} > 2Kx_1^*$, the result follows. □

From Theorem (3), it is clear that E^* is a degenerate singularity. So, now we will study System (7) in the neighborhood of E^*.

Theorem 4. *The equilibrium point E^*, if it exists, is characterized as follows:*

a. A saddle-node when $\frac{K}{\beta^2}((1+m)\beta - 2 + (\beta-1)(1-m\beta)) \neq 0$.

b. A two-codimensional cusp when $\frac{K}{\beta^2}((1+m)\beta - 2 + (\beta-1)(1-m\beta)) = 0$ and $\frac{-2K}{e\beta}(1 + m - \frac{3}{\beta}) - \frac{y^*}{e^2} \neq 0$.

Proof. To shift E^* to the origin, consider the transformation $\hat{x} = x - x^*$, $\hat{y} = y - y^*$, then using Taylor series, System (7) reduces to

$$\begin{aligned} \frac{d\hat{x}}{dt} &= \alpha_{10}\hat{x} + \alpha_{01}\hat{y} + \alpha_{20}\hat{x}^2 + \alpha_{02}\hat{y}^2 + \alpha_{11}\hat{x}\hat{y} + O|(x,y)^3|, \\ \frac{d\hat{y}}{dt} &= \beta_{10}\hat{x} + \beta_{01}\hat{y} + \beta_{20}\hat{x}^2 + \beta_{02}\hat{y}^2 + \beta_{11}\hat{x}\hat{y} + O|(x,y)^3|, \end{aligned} \tag{13}$$

where $\alpha_{10} = \frac{K}{\beta^2}((1+m)\beta - 2 + (\beta-1)(1-m\beta)) = 0$, $\alpha_{01} = -\frac{1}{e\beta}$, $\alpha_{02} = 0$, $\alpha_{11} = 0$, $\alpha_{20} = K(1 + m - \frac{3}{\beta}) + \frac{\beta y^*}{2e}$, $\beta_{10} = 0$, $\beta_{01} = 0$, $\beta_{20} = \frac{-b\beta y^*}{2e}$, $\beta_{02} = 0$, $\beta_{11} = 0$.

Now, the following two cases arise:

a. If $\alpha_{10} \neq 0$, then $Tr(J_{E^*}) \neq 0$ and $det(J_{E^*}) = 0$. So, E^* constitutes a saddle node.

b. If $\alpha_{10} = 0$, then System (13) becomes

$$\begin{aligned} \frac{d\hat{x}}{dt} &= \alpha_{01}\hat{y} + \alpha_{20}\hat{x}^2 + O|(\hat{x},\hat{y})^3|, \\ \frac{d\hat{y}}{dt} &= \beta_{20}\hat{x}^2 + O|(\hat{x},\hat{y})^3|. \end{aligned} \tag{14}$$

After the introduction of the variable $\tau = \alpha_{01}t$, System (14) becomes

$$\begin{aligned} \frac{d\hat{x}}{d\tau} &= \hat{y} + \bar{\alpha}_{20}\hat{x}^2 + O|(\hat{x},\hat{y})^3|, \\ \frac{d\hat{y}}{d\tau} &= \bar{\beta}_{20}\hat{x}^2 + O|(\hat{x},\hat{y})^3|, \end{aligned} \tag{15}$$

where $\bar{\alpha}_{20} = \frac{\alpha_{20}}{\alpha_{01}}$, $\bar{\beta}_{20} = \frac{\beta_{20}}{\alpha_{01}}$.

Taking $z_1 = \hat{x}$, $z_2 = \hat{y} + \bar{\alpha}_{20}\hat{x}^2 + O|(\hat{x},\hat{y})^3|$, System (15) converts to

$$\begin{aligned} \frac{dz_1}{d\tau} &= z_2, \\ \frac{dz_2}{d\tau} &= \bar{\beta}_{20}z_1^2 + 2\bar{\alpha}_{20}z_1z_2 + O|(z_1,z_2)^3|, \end{aligned} \tag{16}$$

where $\bar{\alpha}_{20} = \frac{\alpha_{20}}{\alpha_{01}}$, $\bar{\beta}_{20} = \frac{\beta_{20}}{\alpha_{01}}$.

Now, since $\bar{\beta}_{20} = \frac{by^*}{2e^2} \neq 0$ and if $\bar{\alpha}_{20} = \frac{2}{e\beta(1+n\beta)} - \frac{2n(-1-2n\beta+(m+n+mn)\beta^2)}{e(1+n\beta)^3} + \frac{y^*}{e^2} \neq 0$, then in the z_1z_2 plane, the origin identifies as a cusp of codimension 2, which corresponds to E^* being a 2-codimensional cusp in the xy-plane.

□

4. Bifurcation Analysis

This section accentuates the exploration of diverse bifurcations that System (7) may experience, like saddle-node and Hopf types, both of which are codimension-one bifurcations, and Bogdanov–Taken bifurcation, which is a codimension-two bifurcation.

4.1. Saddle-Node Bifurcation

As noted in Section 3, the unique interior equilibrium point E^* is a result of the coalescing of two interior equilibrium points E_1^* and E_2^* with the variation in the parameter b. The system experiences saddle-node bifurcation as a result of this coalescence. Consider $b = b^{SN} = e\beta d$. Treating b as the bifurcation parameter, we use Sotomayor's theorem to guarantee the emergence of saddle-node bifurcation in System (7).

Theorem 5. *System (7) exhibits the emergence of saddle-node bifurcation around the unique interior equilibrium point $E^* = (x^*, y^*)$, regarding parameter b.*

Proof. One eigenvalue of the Jacobian matrix J_{E^*} is zero due to the fact that $det(J_{E^*}) = 0$. Now, V and W are assumed as two eigenvectors corresponding to the eigenvalue zero of matrix J_{E^*} and $J_{E^*}^T$, respectively, then

$$V = \begin{bmatrix} 1 \\ e\beta(\frac{K}{\beta}(1+m-\frac{2}{\beta})+\frac{y^*}{e}) \end{bmatrix}; W = \begin{bmatrix} 0 \\ 1 \end{bmatrix}.$$

We have

$$W^T F_b(E^*, b^{SN}) = \frac{y^*}{e\beta} \neq 0 \text{ and } W^T[D^2F(E^*, b^{SN})(V,V)] = -\frac{b\beta y^*}{e} \neq 0,$$

where $F_b(E^*, b^{SN}) = \begin{bmatrix} 0 \\ \frac{y^*}{e\beta} \end{bmatrix}$ and $D^2F(E^*, b^{SN}) = \begin{bmatrix} 2K(1+m-\frac{3}{\beta})+\frac{\beta y^*}{e} \\ -\frac{b\beta y^*}{e} \end{bmatrix}$. Thus, the transversality conditions are satisfied. □

To visualize the occurrence of saddle-node bifurcation, we set parameters to $m = 0.1$, $K = 2$, $\beta = 1.1$, and $d = 1$ within System (7); the resulting outcomes including the emergence of saddle-node bifurcation are summarized in Table 1. Corresponding to these parameters, System (7) will showcase two (one stable and the other saddle) interior equilibrium points when b is less than its threshold value. Ecologically, it can be interpreted that under favorable conditions, both species will coexist. When b reaches its threshold value, then one (saddle-node) interior equilibrium point exists. Ecologically, it means that either both species will coexist or prey will go extinct depending on the initial value of the populations. When b crosses its threshold value, then a zero interior equilibrium point exists. In this case, either prey will go extinct or both species will cease to exist depending on the initial value of the populations.

Table 1. Saddle-node bifurcation.

b	Equilibrium Points		Figure
	Boundary	**Interior**	
$0 < b < b^{SN} = 2.99011$	$E_0 = (0,0)$, $E_1 = (1,0)$, $E_2 = (0.1,0)$	$E_1^* = (0.8372, 0.602865)$, $E_2^* = (0.984984, 0.0785358)$	Figure 3a
$b = b^{SN}$		$E^* = (0.909091, 0.399879)$ emergence of saddle-node bifurcation	Figure 3b,d
$b > b^{SN}$		None	Figure 3c

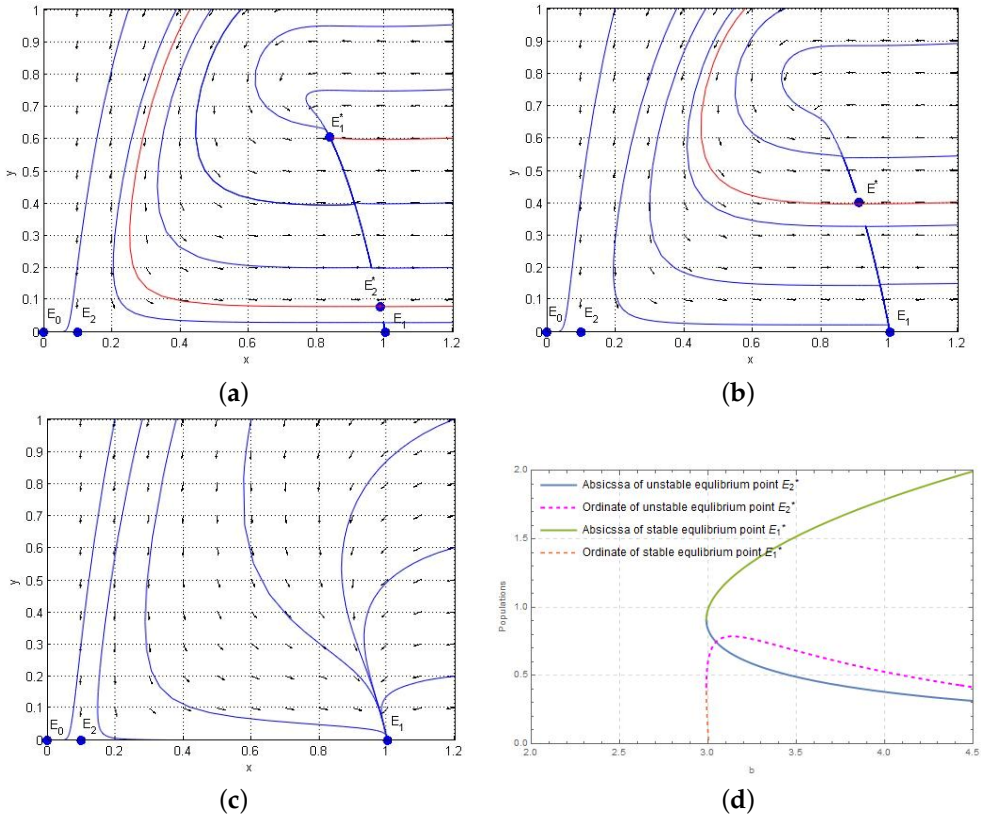


Figure 3. Equilibrium points exhibited by System (7). The arrows depict the direction of the solution trajectories. (**a**) At $b = 3$. (**b**) At $b = b^{SN} = 2.99011$. (**c**) At $b = 2$. (**d**) Saddle-node bifurcation diagram.

4.2. Hopf Bifurcation

Evidently, from Section 3, E_2^*, if existent, is invariably a saddle point. Also, E_1^*, if existent, is stable under the condition $\frac{1}{K}(2Kx_1^* - K - \beta y_1^* e^{-\beta x_1^*}) > m$. Also, $det(J_{E_1^*}) > 0$ and $Tr(J_{E_1^*}) = 0$ when $\frac{1}{K}(2Kx_1^* - K - \beta y_1^* e^{-\beta x_1^*}) = m$. Then, the nature of eigenvalues of $J_{E_1^*}$ is purely imaginary. Therefore, E_1^* will emerge as either a center or a weak focus.

Theorem 6. *System* (7) *experiences the emergence of Hopf bifurcation at the interior equilibrium point* E_1^*, *when* $m = m^{hf} = \frac{1}{K}(2Kx_1^* - K - \beta y_1^* e^{-\beta x_1^*})$, *with the direction as supercritical or subcritical depending on the sign of* Λ.

Proof. Consider m as the bifurcation parameter; then, for the threshold value $m = m^{hf} = \frac{1}{K}(2Kx_1^* - K - \beta y_1^* e^{-\beta x_1^*})$, we have $det(J_{E_1^*}) > 0$, $Tr(J_{E_1^*}) = 0$, and $\frac{\partial}{\partial m}(Tr(J_{E_1^*})) = Kx_1^* \neq 0$. Now, as a result of Hopf bifurcation, the system will experience the rise of a limit cycle. For exploration of the stability of the emergent limit cycles, we find the Lyapunov number. Firstly, to shift $E_1^* = (x_1^*, y_1^*)$ to the origin, we consider coordinate transformation $\hat{x} = x - x_1^*$, $\hat{y} = y - y_1^*$. Thus, System (7) is reduced to (retaining x and y in place of $\hat{x}$ and $\hat{y}$, respectively)

$$\begin{aligned} \frac{dx}{dt} &= \alpha_{10}x + \alpha_{01}y + \alpha_{20}x^2 + \alpha_{11}xy + \alpha_{02}y^2 + \alpha_{30}x^3 + \alpha_{03}y^3 + \alpha_{21}x^2y + \alpha_{12}xy^2 + H(x,y), \\ \frac{dy}{dt} &= \beta_{10}x + \beta_{01}y + \beta_{20}x^2 + \beta_{11}xy + \beta_{02}y^2 + \beta_{30}x^3 + \beta_{03}y^3 + \beta_{21}x^2y + \beta_{12}xy^2 + G(x,y), \end{aligned} \tag{17}$$

where $\alpha_{10} = Kx(1+m-2x) + K(1-x)(x-m) - ye^{-\beta x}(1-\beta x)$, $\alpha_{01} = -xe^{-\beta x}$, $\alpha_{20} = -Kx + Kx(1+m-2x) + \frac{y\beta e^{-\beta x}(2-\beta x)}{2}$, $\alpha_{11} = -e^{-\beta x}(1-\beta x)$, $\alpha_{02} = 0$, $\alpha_{30} = -K - \frac{\beta^2 y e^{-\beta x}(3-\beta x)}{6}$, $\alpha_{03} = 0$, $\alpha_{21} = \frac{\beta e^{-\beta x}(2-\beta x)}{2}$, $\alpha_{12} = 0$, $\beta_{10} = bye^{-\beta x}(1-\beta x)$, $\beta_{01} = bxe^{-\beta x} - d$, $\beta_{20} = \frac{-b\beta y e^{-\beta x}(2-\beta x)}{2}$, $\beta_{02} = 0$, $\beta_{11} = be^{-\beta x}(1-\beta x)$, $\beta_{30} = \frac{b\beta^2 y e^{-\beta x}(3-\beta x)}{6}$, $\beta_{03} = 0$, $\beta_{21} = \frac{-b\beta e^{-\beta x}(2-\beta x)}{2}$, $\beta_{12} = 0$ and H, and G is a power series in (x, y) with powers x^i, y^j satisfying $i + j \geq 4$.

At the origin, the first Lyapunov number is

$$\begin{aligned}\Lambda = (3\pi e^{-3\beta x}(b\beta x^2 y(\beta x-2)(b(\beta x-1)+2k(-m+3x-1)e^{\beta x}+\beta y(2-\beta x))-\\ (bxy(\beta x-1)+(k(-2mx+m+x(3x-2))e^{\beta x}-\beta xy+y)^2)(\beta(bx(\beta x-2)-\\ y(\beta^2x^2-3\beta x+4))+2ke^{\beta x}(-2\beta m-2\beta x^2(\beta+\beta m+3)+x(\beta^2 m+4\beta(m+1)-\\ 3)+3\beta^2x^3))+2by(\beta x-1)^3(k(-2mx+m+x(3x-2))e^{\beta x}-\beta xy+y)+bx(\beta x-1)\\ (k(-2mx+m+x(3x-2))e^{\beta x}-\beta xy+y)(2b(\beta x-1)+2k(-m+3x-1)e^{\beta x}+\\ \beta y(2-\beta x))+2e^{\beta x}(1-\beta x)(k(m-3x+1)+\frac{1}{2}\beta y e^{\beta(-x)}(\beta x-2))(bxy(\beta x-1)-2(k\\ (-2mx+m+x(3x-2))e^{\beta x}-\beta xy+y)^2)-x(k(-2mx+m+x(3x-2))e^{\beta x}-\beta xy+y)\\ (2k(-m+3x-1)e^{\beta x}+\beta y(2-\beta x))^2))/(4x(e^{\beta(-x)}(d(k(-2mx+m+x(3x-2))e^{\beta x}\\ -\beta xy+y)-bkx(-2mx+m+x(3x-2))))^{3/2})\end{aligned}$$

If $\Lambda > 0$, then subcritical Hopf bifurcation appears around the point, E_1^* and if $\Lambda < 0$, then supercritical Hopf bifurcation appears around the point E_1^*. □

To visualize the occurrence of Hopf bifurcation, we set parameters to $K = 2$, $b = 3$, $\beta = 1.1$, and $d = 1$ within System (7); the resulting outcomes, including the emergence of a limit cycle, are summarized in Table 2. Corresponding to these parameters, System (7) will always showcase two interior equilibrium points, but their nature will change depending on the parameter m. One of these equilibrium points will always be a saddle, while the other can appear as unstable, surrounded by a stable limit cycle or stable. Ecologically, it means that either prey will go extinct, the system will collapse altogether, oscillating behavior will be exhibited, or both species will coexist contingent on the Allee effect parameter and initial values that the system commences with.

Table 2. Emergence of Hopf bifurcation.

m	Equilibrium Points		Figure
	Boundary	**Interior**	
$m = 0.4$	$E_0 = (0,0)$ (stable), $E_1 = (1,0)$ (stable), $E_2 = (0.4,0)$ (saddle)	$E_1^* = (0.8372, 0.357532)$ (unstable), $E_2^* = (0.984984, 0.051913)$ (saddle)	Figure 4a
$m = m^{hf} = 0.638886$	$E_0 = (0,0)$ (stable), $E_1 = (1,0)$ (stable), $E_2 = (0.287845,0)$ (saddle)	Stable limit cycle (as $\Lambda < 0$) around $E_1^* = (0.8372, 0.162177)$ (stable), $E_2^* = (0.984984, 0.0307137)$ (saddle)	Figure 4b
$m = 0.7$	$E_0 = (0,0)$ (stable), $E_1 = (1,0)$ (stable), $E_2 = (0.1,0)$ (saddle)	$E_1^* = (0.8372, 0.112199)$ (stable), $E_2^* = (0.984984, 0.0252902)$ (saddle)	Figure 4c

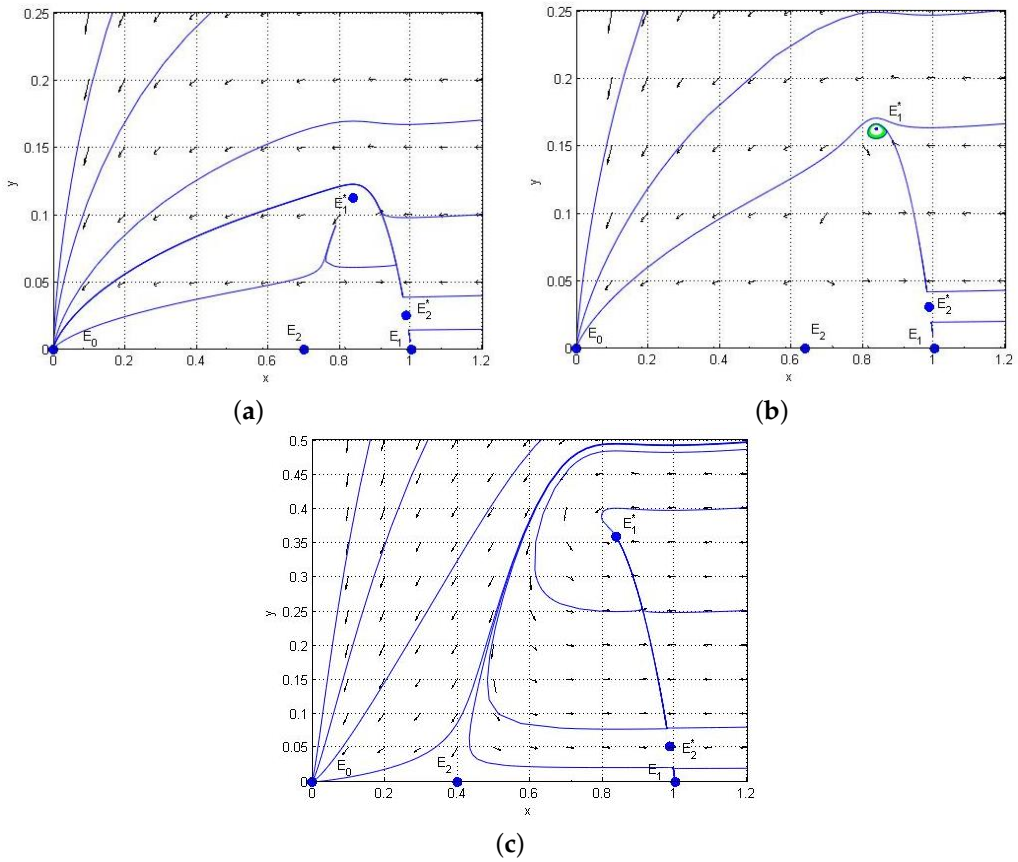


Figure 4. Equilibrium points exhibited by System (7). The arrows depict the direction of the solution trajectories. (**a**) At $m = 0.4$, E_2^* is continuously a saddle and E_1^* is unstable. (**b**) At $m = m^{hf} = 0.638886$, E_1^* is enclosed by a stable limit cycle. (**c**) At $m = 0.7$, E_1^* is stable.

4.3. Bogdanov–Takens (B-T) Bifurcation

The emergence of B-T bifurcation in System (7) is a result of the intersection of the Hopf bifurcation curve and the saddle-node bifurcation curve in the bi-parameter bifurcation plane. From a mathematical point of view, B-T bifurcation occurs at critical parametric values corresponding to which both eigenvalues of the Jacobian matrix are zero.

Theorem (4) clearly demonstrates that E^* is a cusp of codimension two, when $\frac{K}{\beta^2}((1+m)\beta - 2 + (\beta-1)(1-m\beta)) = 0$, $\frac{by^*}{2e^2} \neq 0$ and $\frac{-2K}{e\beta}(1+m-\frac{3}{\beta}) - \frac{y^*}{e^2} \neq 0$. Designating m and b as the bifurcation parameters, we proceed to explore the emergence of Bogdanov-Taken bifurcation.

Theorem 7. *Codimension-two B-T bifurcation is experienced by System* (7) *around the equilibrium point* $E^* = (x^*, y^*)$*, with regard to parameters m and b, whenever* $\frac{K}{\beta^2}((1+m)\beta - 2 + (\beta-1)(1-m\beta)) = 0$, $\frac{by^*}{2e^2} \neq 0$ *and* $\frac{-2K}{e\beta}(1+m-\frac{3}{\beta}) - \frac{y^*}{e^2} \neq 0$.

Proof. We proceed with the analysis under the assumption that bifurcation parameters m and b undergo small variation within the vicinity of the BT-point (intersection of saddle-node and Hopf bifurcation curves) (m_0, b_0). Consider a point $(m_0 + \lambda_1, b_0 + \lambda_2)$ near the BT-point (m_0, b_0), where λ_1 and λ_2 are small. Then, System (7) becomes

$$\begin{aligned} \frac{dx}{dt} &= x(K(1-x)(x-(m+\lambda_1)) - ye^{-\beta x}), \\ \frac{dy}{dt} &= y((b+\lambda_2)xe^{-\beta x} - d), \end{aligned} \tag{18}$$

System (18), in regard to the variables x and y, exhibits C^∞ smoothness in the vicinity of (m_0, b_0).

Taking $u = x - x^*$, $v = y - y^*$, System (18) turns into

$$\begin{aligned} \frac{du}{dt} &= \alpha_{00} + \alpha_{10}u + \alpha_{01}v + \alpha_{20}u^2 + \alpha_{11}uv + \alpha_{02}v^2 + R_1(u,v), \\ \frac{dv}{dt} &= \beta_{00} + \beta_{10}u + \beta_{01}v + \beta_{20}u^2 + \beta_{11}uv + \beta_{02}v^2 + R_2(u,v), \end{aligned} \tag{19}$$

where $\alpha_{00} = \frac{-\lambda_1 K(\beta-1)}{\beta^2}$, $\alpha_{10} = \frac{K}{\beta^2}((1+m+\lambda_1)\beta - 2 + (\beta-1)(1-\beta(m+\lambda_1)))$, $\alpha_{01} = \frac{-1}{e\beta}$, $\alpha_{20} = \frac{2K}{\beta}((1+m+\lambda_1)\beta - 3) + \frac{y^*\beta}{e}$, $\alpha_{11} = 0$, $\alpha_{02} = 0$, $\beta_{00} = \frac{\lambda_2 y^*}{e\beta}$ $\beta_{10} = 0$, $\beta_{01} = \frac{\lambda_2}{e\beta}$, $\beta_{20} = \frac{-(b+\lambda_2)\beta y^*}{2e}$, $\beta_{02} = 0$, $\beta_{11} = 0$, and R_1, R_2 is a power series in (u, v) with powers u^i, v^j satisfying $i + j \geq 3$, and the coefficients smoothly depend upon λ_1 and λ_2.

Next, using the affine transformation $y_1 = u$, $y_2 = \alpha_{10}u + \alpha_{01}v$, System (19) becomes

$$\begin{aligned} \frac{dy_1}{dt} &= y_2 + \xi_{00} + \xi_{20}y_1^2 + \tilde{R}_1(y_1, y_2), \\ \frac{dy_2}{dt} &= \eta_{00} + \eta_{10}y_1 + \eta_{01}y_2 + \eta_{20}y_1^2 + \tilde{R}_2(y_1, y_2), \end{aligned} \tag{20}$$

where $\xi_{00} = \alpha_{00}$, $\xi_{20} = \alpha_{20}$, $\eta_{00} = \alpha_{00}\alpha_{10} + \beta_{00}\alpha_{01}$, $\eta_{10} = -\alpha_{10}\beta_{01}$, $\eta_{01} = \alpha_{10} + \beta_{01}$, $\eta_{20} = \alpha_{20}\alpha_{10} + \alpha_{01}\beta_{20}$, and $\tilde{R}_1$,$\tilde{R}_2$ is a power series in (y_1, y_2) with powers y_1^i, y_2^j satisfying $i + j \geq 3$, and the coefficients smoothly depend upon λ_1 and λ_2.

Next, we perform the C^∞ transformations $z_1 = y_1$, $z_2 = y_2 + \xi_{00} + \xi_{20}y_1^2$; then, System (20) becomes

$$\begin{aligned} \frac{dz_1}{dt} &= z_2 + \hat{R}_1(z_1, z_2), \\ \frac{dz_2}{dt} &= \gamma_{00} + \gamma_{10}z_1 + \gamma_{01}z_2 + \gamma_{20}z_1^2 + \gamma_{11}z_1z_2 + \hat{R}_2(z_1, z_2), \end{aligned} \tag{21}$$

where $\gamma_{00} = \eta_{00} - \xi_{00}\eta_{01}$, $\gamma_{10} = \eta_{10}$, $\gamma_{01} = \eta_{01}$, $\gamma_{20} = \eta_{20} - \xi_{20}\eta_{01}$, $\gamma_{11} = 2\xi_{20}$, and $\hat{R}_1$,$\hat{R}_2$ is a power series in (z_1, z_2) with powers z_1^i, z_2^j satisfying $i + j \geq 3$, and the coefficients smoothly depend upon λ_1 and λ_2.

The sign of γ_{20} is hard to establish when λ_1 and λ_2 are small. So, it is important to consider the following cases:

Case 1: $\gamma_{20} > 0$

Consider $U = z_1$, $V = \frac{z_2}{\sqrt{\gamma_{20}}}$, $d\tau = \sqrt{\gamma_{20}}dt$; then, System (21) becomes

$$\begin{aligned} \frac{dU}{d\tau} &= V, \\ \frac{dV}{d\tau} &= p_{00} + p_{10}U + p_{01}V + U^2 + p_{11}UV + R_3(U, V), \end{aligned} \tag{22}$$

where $p_{00} = \frac{\gamma_{00}}{\gamma_{20}}$, $p_{10} = \frac{\gamma_{10}}{\gamma_{20}}$, $p_{01} = \frac{\gamma_{01}}{\sqrt{\gamma_{20}}}$, $p_{11} = \frac{\gamma_{11}}{\sqrt{\gamma_{20}}}$, and R_3 is a power series in (U, V) with powers U^i, V^j satisfying $i + j \geq 3$, and the coefficients smoothly depend upon λ_1 and λ_2.

Next, we use the affine transformation $v_1 = U + \frac{p_{10}}{2}$, $v_2 = V$; System (22) becomes

$$\begin{aligned} \frac{dv_1}{d\tau} &= v_2, \\ \frac{dv_2}{d\tau} &= q_{00} + q_{01}v_2 + v_1^2 + q_{11}v_1v_2 + R_4(v_1, v_2), \end{aligned} \tag{23}$$

where $q_{00} = p_{00} - \frac{p_{10}^2}{4}$, $q_{01} = p_{01} - \frac{p_{11}p_{10}}{2}$, $q_{11} = p_{11}$, and R_4 is a power series in (v_1, v_2) with powers v_1^i, v_2^j satisfying $i + j \geq 3$, and the coefficients smoothly depend upon λ_1 and λ_2.

By changing the variables $w_1 = q_{11}^2 v_1$, $w_2 = q_{11}^3 v_2$, $t = \frac{\tau}{q_{11}}$, System (23) becomes

$$\begin{aligned} \frac{dw_1}{dt} &= w_2, \\ \frac{dw_2}{dt} &= \zeta_1(\lambda_1, \lambda_2) + \zeta_2(\lambda_1, \lambda_2) w_2 + w_1^2 + w_1 w_2 + R_5(w_1, w_2), \end{aligned} \tag{24}$$

where

$$\zeta_1(\lambda_1, \lambda_2) = q_{00} q_{11}^4, \ \zeta_2(\lambda_1, \lambda_2) = q_{01} q_{11} \tag{25}$$

and R_5 is a power series in (w_1, w_2) with powers w_1^i, w_2^j satisfying $i + j \geq 3$, and the coefficients smoothly depend upon λ_1 and λ_2.

Case 2: $\gamma_{20} < 0$

Consider $\bar{U} = z_1$, $\bar{V} = \frac{z_2}{\sqrt{-\gamma_{20}}}$, $d\tau = \sqrt{-\gamma_{20}} dt$; then, System (21) becomes

$$\begin{aligned} \frac{d\bar{U}}{d\tau} &= \bar{V}, \\ \frac{d\bar{V}}{d\tau} &= \bar{p}_{00} + \bar{p}_{10}\bar{U} + \bar{p}_{01}\bar{V} + \bar{U}^2 + \bar{p}_{11}\bar{U}\bar{V} + \bar{R}_3(\bar{U}, \bar{V}), \end{aligned} \tag{26}$$

where $\bar{p}_{00} = \frac{-\gamma_{00}}{\gamma_{20}}$, $\bar{p}_{10} = \frac{-\gamma_{10}}{\gamma_{20}}$, $\bar{p}_{01} = \frac{\gamma_{01}}{\sqrt{-\gamma_{20}}}$, $\bar{p}_{11} = \frac{\gamma_{11}}{\sqrt{-\gamma_{20}}}$, and $\bar{R}_3$ is a power series in $(\bar{U}, \bar{V})$ with powers $\bar{U}^i, \bar{V}^j$ satisfying $i + j \geq 3$, and the coefficients smoothly depend upon λ_1 and λ_2.

Next, we use affine transformation $\bar{v}_1 = \bar{U} - \frac{\bar{p}_{10}}{2}$, $\bar{v}_2 = \bar{V}$; System (26) becomes

$$\begin{aligned} \frac{d\bar{v}_1}{d\tau} &= \bar{v}_2, \\ \frac{d\bar{v}_2}{d\tau} &= \bar{q}_{00} + \bar{q}_{01}\bar{v}_2 + \bar{v}_1^2 + \bar{q}_{11}\bar{v}_1\bar{v}_2 + \bar{R}_4(\bar{v}_1, \bar{v}_2), \end{aligned} \tag{27}$$

where $\bar{q}_{00} = \bar{p}_{00} + \frac{\bar{p}_{10}^2}{4}$, $\bar{q}_{01} = \bar{p}_{01} + \frac{\bar{p}_{11}\bar{p}_{10}}{2}$, $\bar{q}_{11} = \bar{p}_{11}$, and $\bar{R}_4$ is a power series in $(\bar{v}_1, \bar{v}_2)$ with powers $\bar{v}_1^i, \bar{v}_2^j$ satisfying $i + j \geq 3$, and the coefficients smoothly depend upon λ_1 and λ_2.

Consider new variables $\bar{w}_1 = -\bar{q}_{11}^2 \bar{v}_1$, $\bar{w}_2 = \bar{q}_{11}^3 \bar{v}_2$, $t = -\frac{\tau}{\bar{q}_{11}}$; System (27) becomes

$$\begin{aligned} \frac{d\bar{w}_1}{dt} &= \bar{w}_2, \\ \frac{d\bar{w}_2}{dt} &= \bar{\zeta}_1(\lambda_1, \lambda_2) + \bar{\zeta}_2(\lambda_1, \lambda_2)\bar{w}_2 + \bar{w}_1^2 + \bar{w}_1\bar{w}_2 + \bar{R}_5(\bar{w}_1, \bar{w}_2), \end{aligned} \tag{28}$$

where

$$\bar{\zeta}_1(\lambda_1, \lambda_2) = -\bar{q}_{00}\bar{q}_{11}^4, \ \bar{\zeta}_2(\lambda_1, \lambda_2) = -\bar{q}_{01}\bar{q}_{11} \tag{29}$$

and $\bar{R}_5$ is a power series in $(\bar{w}_1, \bar{w}_2)$ with powers $\bar{w}_1^i, \bar{w}_2^j$ satisfying $i + j \geq 3$, and the coefficients smoothly depend upon λ_1 and λ_2.

In (29), $\bar{\zeta}_1(\lambda_1, \lambda_2)$ and $\bar{\zeta}_2(\lambda_1, \lambda_2)$ can be symbolized using $\zeta_1(\lambda_1, \lambda_2)$ and $\zeta_2(\lambda_1, \lambda_2)$ to reduce the number of cases. In the vicinity of the origin, the parameter transformations in (25) and (29) are topologically equivalent if $\left| \frac{\partial(\zeta_1, \zeta_2)}{\partial(\lambda_1, \lambda_2)} \right|_{\lambda_1 = \lambda_2 = 0}$ is non-singular. From this, the interpretation can be drawn that when (λ_1, λ_2) are in the vicinity of the origin, emergence of Bogdanov–Takens bifurcation occurs within System (18) (cf. Perko [30]). The bifurcation curves are as follows:

1. The saddle-node bifurcation curve:
   $SN = (\lambda_1, \lambda_2) : \zeta_1(\lambda_1, \lambda_2) = 0, \zeta_2(\lambda_1, \lambda_2) \neq 0$;
2. The Hopf bifurcation curve:
   $H = (\lambda_1, \lambda_2) : \zeta_2(\lambda_1, \lambda_2) = \pm\sqrt{-\zeta_1(\lambda_1, \lambda_2)}, \zeta_1(\lambda_1, \lambda_2) < 0$;
3. The homoclinic bifurcation curve:
   $HL = (\lambda_1, \lambda_2) : \zeta_2(\lambda_1, \lambda_2) = \pm\frac{5}{7}\sqrt{-\zeta_1(\lambda_1, \lambda_2)}, \zeta_1(\lambda_1, \lambda_2) < 0$.

□

To visualize the occurrence of saddle-node bifurcation, we set parameters to $K = 2$, $\beta = 1.1$, and $d = 1$ within System (7); we start by finding threshold values, $m_0 = 0.808081$ and $b_0 = 2.99011$. A unique interior equilibrium point $E^* = (0.909091, 0.0499225)$ emerges in System (7), corresponding to these parameters. By integrating all these parameters, we derive the subsequent system

$$\begin{aligned} \frac{dx}{dt} &= 2x(1-x)(x-(0.808081+\lambda_1)) - xye^{-1.1x}, \\ \frac{dy}{dt} &= y((2.99011+\lambda_2)xe^{-1.1x} - 1), \end{aligned} \tag{30}$$

System (30) exhibits C^∞ smoothness in the vicinity of (m_0, b_0) with respect to variables x and y.

Now, we use three transformations in sequence, first to shift the equilibrium point to the origin, $u = x - 0.909091$, $v = y - 0.0499225$, then the affine transformation $y_1 = u$, $y_2 = \alpha_{10}u + \alpha_{01}v$, and lastly the C^∞ transformations $z_1 = y_1$, $z_2 = y_{2+} + \xi_{00} + \xi_{20}y_1^2$, then System (30) becomes

$$\begin{aligned} \frac{dz_1}{dt} &= z_2 + \hat{R}_1(z_1, z_2), \\ \frac{dz_2}{dt} &= \gamma_{00} + \gamma_{10}z_1 + \gamma_{01}z_2 + \gamma_{20}z_1^2 + \gamma_{11}z_1z_2 + \hat{R}_2(z_1, z_2), \end{aligned} \tag{31}$$

where $\gamma_{00} = 0.0552787(\lambda_1\lambda_2 - 2.229785060294064 \times 10^{-31}\lambda_1 - 0.10101\lambda_2)$, $\gamma_{10} = -0.547259$ $(2.55828 \times 10^{-16} + \lambda_1)\lambda_2$, $\gamma_{01} = 1.63636(2.55828 \times 10^{-16} + \lambda_1 + 0.204377\lambda_2)$, $\gamma_{20} = -1.33774$ $(-0.00755078 - 0.916667\lambda_2 + \lambda_1\lambda_2)$, $\gamma_{11} = 8(-0.914141 + \lambda_1)$, and $\hat{R}_1$,$\hat{R}_2$ is a power series in (z_1, z_2) with powers z_1^i, z_2^j satisfying $i + j \geq 3$, and the coefficients smoothly depend upon λ_1 and λ_2.

When λ_1 and λ_2 are small, we have $\gamma_{20} = 0.010101$. So, next, we make transformation $U = z_1$, $V = \frac{z_2}{\sqrt{\gamma_{20}}}$, $d\tau = \sqrt{\gamma_{20}}dt$, then we consider affine transformation $v_1 = U + \frac{p_{10}}{2}$, $v_2 = V$, and lastly, we change the variables $w_1 = q_{11}^2 v_1$, $w_2 = q_{11}^3 v_2$, $t = \frac{\tau}{q_{11}}$; System (31) becomes

$$\begin{aligned} \frac{dw_1}{dt} &= w_2, \\ \frac{dw_2}{dt} &= \zeta_1(\lambda_1, \lambda_2) + \zeta_2(\lambda_1, \lambda_2)w_2 + w_1^2 + w_1w_2 + R_5(w_1, w_2), \end{aligned} \tag{32}$$

where

$$\zeta_1(\lambda_1, \lambda_2) = q_{00}q_{11}^4, \zeta_2(\lambda_1, \lambda_2) = q_{01}q_{11}, \tag{33}$$

$q_{00} = -((0.0831612(8.36602 \times 10^{-34}\lambda_1 + 0.000378984\lambda_2 - 0.00375194\lambda_1\lambda_2 - 1.10797 \times 10^{-31}\lambda_1^2\lambda_2 + 0.0460087\lambda_2^2 - 0.505678\lambda_1\lambda_2^2 + \lambda_1^2\lambda_2^2))/(-0.00755078 - 0.916667\lambda_2 + \lambda_1\lambda_2)^2)$, $q_{01} = (0.289152(-9.45163 \times 10^{-18} - 0.0369453\lambda_1 - 0.00755078\lambda_2 - 0.0123558\lambda_1\lambda_2 - 7.67916 \times 10^{-16}\lambda_1^2\lambda_2 - 0.916667\lambda_2^2 + \lambda_1\lambda_2^2))/(Sqrt[0.00755078 + 0.916667\lambda_2 - \lambda_1\lambda_2]$ $(-0.00755078 - 0.916667\lambda_2 + \lambda_1\lambda_2))$, $q_{11} = (6.91677(-0.914141 + \lambda_1))/Sqrt[0.00755078 +$

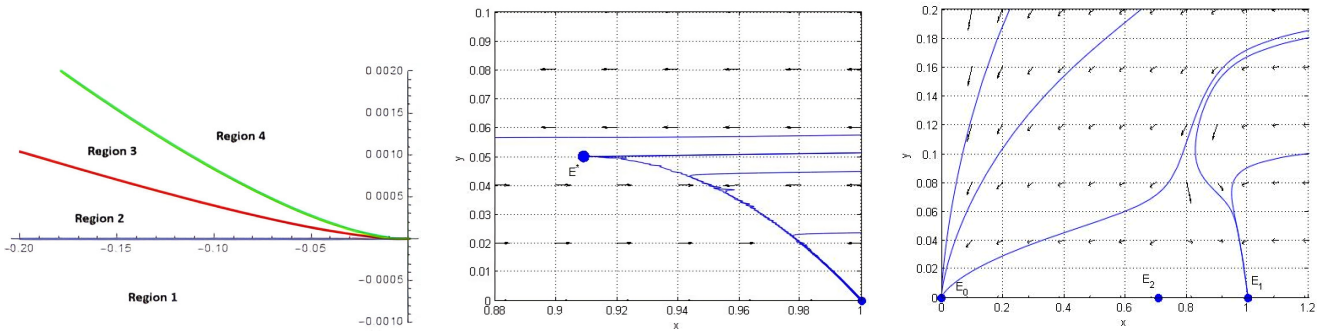
$0.916667\lambda_2 - \lambda_1\lambda_2]$ and R_5 is a power series in (w_1, w_2) with powers w_1^i, w_2^j satisfying $i + j \geq 3$, and the coefficients smoothly depend upon λ_1 and λ_2.

The determinant $E = \left|\frac{\partial(\zeta_1,\zeta_2)}{\partial(\lambda_1,\lambda_2)}\right|_{\lambda_1=\lambda_2=0} = -1.83595 * 10^{10} \neq 0$, which implies matrix E has rank 2, and this leads to the parametric transformation (33) being non-singular. In the vicinity of the BT point $(0, 0)$, the three bifurcation curves divide the bi-parameter bifurcation plane $\lambda_1\lambda_2$ into four distinct regions (ref. Figure 5a). The saddle-node bifurcation curve is depicted in blue, the Hopf bifurcation curve in red, and the homoclinic bifurcation curve in green.

System (30) possesses a single coexistence equilibrium point, when $\lambda_1 = \lambda_2 = 0$, and it constitutes a codimension-two cusp (Figure 5b). To enter Region 1, values of λ_1 and λ_2 are varied; here, the absence of an interior equilibrium point is noted in System (30). The implication of this is that the system will move towards a prey-free equilibrium point (Figure 5c). Transitioning into Region 2 by varying λ_1 and λ_2, the state of the system changes as it transitions from having zero to two coexistence equilibrium points. One of the equilibrium points is stable while the other is consistently saddle, as shown in Figure 5d. As values of λ_1 and λ_2 enter Region 3, crossing the Hopf bifurcation curve, an unstable limit cycle encloses the positive equilibrium point, as shown in Figure 5e. By varying the values of λ_1 and λ_2 as the system enters Region 4, the loss of the limit cycle is noted, and a coexistence equilibrium point that is unstable along with a saddle coexistence equilibrium point is attained (Figure 5f). The behavior of various regions are given in detail in table 3.

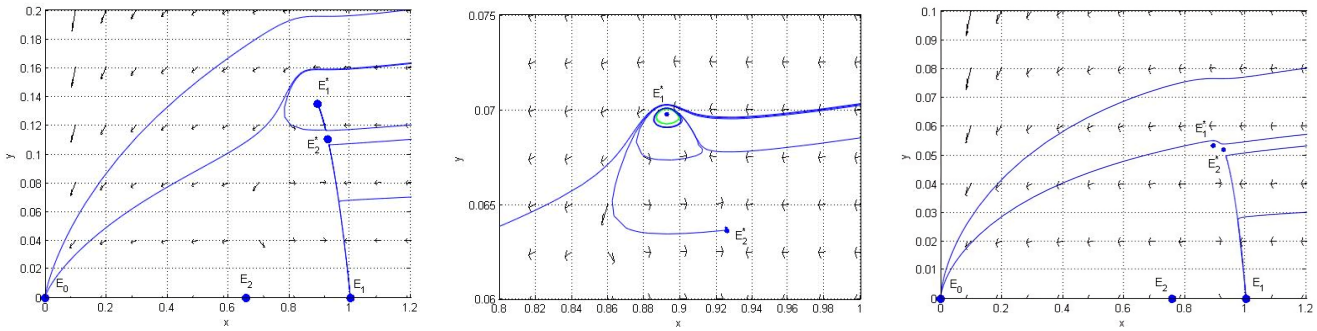
Table 3. Behavior of the system in various regions.

Region	Number of Interior Equilibrium Points	Description of Dynamic Behavior	Figure
Origin	One	Cusp	Figure 5b
First	Zero		Figure 5c
Second	Two	One remains saddle while other exudes stability	Figure 5d
Third	Two	One remains saddle while limit cycle surrounds the other	Figure 5e
Fourth	Two	One remains saddle while other emerges as unstable	Figure 5f



(**a**) (**b**) (**c**)

Figure 5. *Cont.*



(**d**) (**e**) (**f**)

Figure 5. (**a**) Bogdanov–Takens bifurcation diagram. The blue curves represent the solution trajectories of the system and the arrows depict the direction of these trajectories in (**b**–**f**). (**b**) At $\lambda_1 = \lambda_2 = 0$, the cusp appears. (**c**) Region 1: Absence of coexistence equilibrium point. (**d**) Region 2: Two coexistence equilibrium points (one saddle and the other stable). (**e**) Region 3: Two coexistence equilibrium points (one surrounded by a stable limit cycle and the other saddle). (**f**) Region 4: Two coexistence equilibrium points (one saddle and the other unstable).

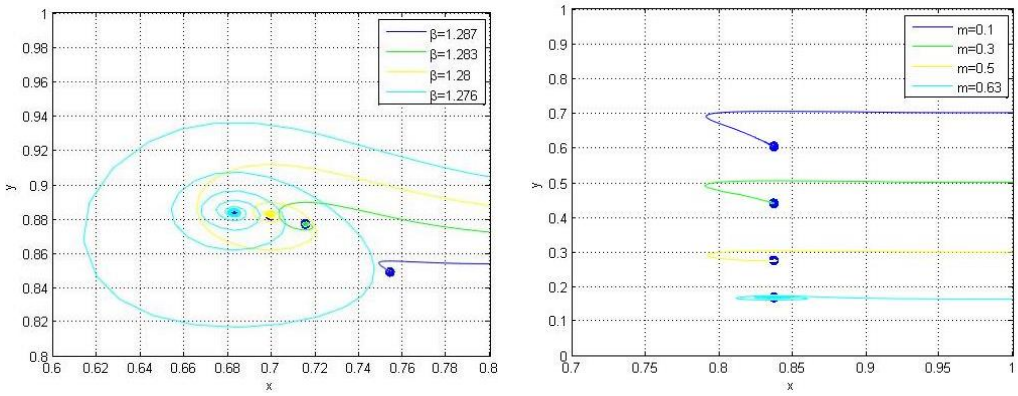
5. Impact of Group Defense and Multiplicative Allee Effect

In this section, we aim to study how the multiplicative Allee effect and group defense influence $E_1^* = (x_1^*, y_1^*)$, where $0 < x_1^* < \frac{1}{\beta}$ and $y_1^* = Ke^{\beta x_1^*}(1 - x_1^*)(x_1^* - m)$, which is stable under the condition $K + mK + \beta y_1^* e^{-\beta x_1^*} < 2Kx_1^*$.

Clearly, x_1^* is independent of m, so the multiplicative Allee effect has no direct impact on the abscissa x_1^*. Further,

$$\frac{dy_1^*}{dm} = -Ke^{-\beta x_1^*}(1 - x_1^*)$$

implies that the ordinate y_1^* is a decreasing function of m. That means an increase in the Allee effect parameter m leads to a decrease in the predator population, at which the stable equilibrium point is obtained, while the corresponding prey population remains unchanged (see Figure 6a).



(**a**) (**b**)

Figure 6. (**a**) Impact of m on E_1^*. (**b**) Impact of β on E_1^*.

Moving on to study the effect of group defense on equilibrium point E_1^*, we can see that the range for x_1^* is $0 < x_1^* < \frac{1}{\beta}$ and y_1^* depends on β. And

$$\frac{dy_1^*}{d\beta} = -Kx_1^* e^{-\beta x_1^*}(1 - x_1^*)(x_1^* - m)$$

indicating that y_1^* is a decreasing function of β and as β increases, the range for x_1^* decreases, so the value of x_1^* decreases. That means as the group defense parameter β is increased, the

prey population decreases and becomes significantly small, while the predator population increases, when the interior equilibrium point E_1^* is stable (see Figure 6b).

Now, to see the combined impact of the multiplicative Allee effect parameter and group defense parameter, we plot the ordinate of equilibrium point E_1^* with m and β simultaneously (Figure 7). It is depicted that as m and β increase, the predator population corresponding to stable equilibrium point E_1^* decreases.

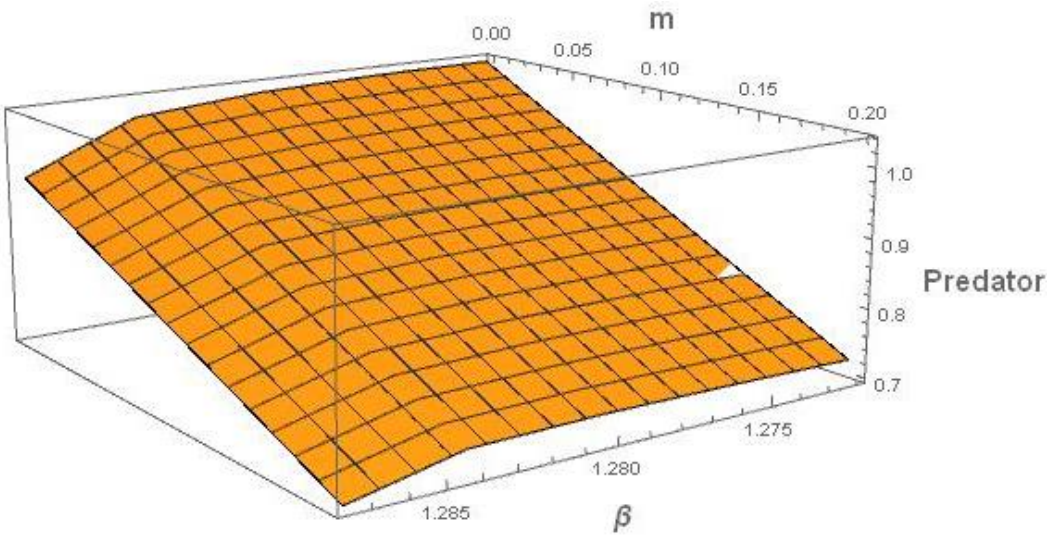


Figure 7. Impact of m and β on predator population y_1^* corresponding to equilibrium point E_1^*.

6. Concluding Observations

The agenda of this article is to delve into the qualitative study of predator–prey interaction in the presence of group defense along with the integration of the multiplicative Allee effect. The analysis of the dynamics of the proposed system is conducted by performing a stability and bifurcation analysis of all ecologically valuable equilibrium points. The first step is to examine the well-posedness of the system. Following this, all feasible equilibrium points and the parametric conditions under which they exist are calculated. The fact that the system invariably exhibits three axial equilibrium points, E_0, E_1, and E_2, was established. Also, depending on the parameter b, the system evinces zero, one (E^*), or two (E_1^*, E_2^*) interior equilibrium points. The stability computation pointed out that the extinction equilibrium point E_0 is invariably stable, the equilibrium point E_1 switches between the state of being a stable point or a saddle point contingent on parametric conditions, and E_2 will either be unstable or saddle based on specific parametric restrictions. When the system possesses two interior equilibrium points, E_1^* will toggle between being stable, unstable, or enclosed within a stable limit cycle based on the parametric restrictions while E_2^* is invariably a saddle point. When the system possesses a unique interior equilibrium point, then it will either constitute a saddle node or a cusp of codimension two based on the parametric conditions. From an ecological perspective, it can be concluded that both species will coexist, prey will go extinct, oscillating behavior will be exhibited by the species, or the system will collapse altogether. The behavior of the system is significantly reliant on the initial population of prey and predator. Following the establishment of equilibrium points and performing the stability analysis, the identification of various bifurcations of codimension one like saddle-node and Hopf bifurcation, and codimension two like Bogdanov–Takens bifurcation, emerging in the system has been achieved. The emergence of saddle-node bifurcation in a system signifies variation in the number of coexistence equilibrium points, driven by variations in the parameter value. This shift can result in significant complex ecological events like species extinction or persistence. The emergence of Hopf bifurcation

indicates that the coexistence of species' populations follows a cyclic pattern over time. The emergence of Bogdanov–Takens bifurcation indicates that different parametric values lead to different ways in which the two species can exist. All these results are validated using both analytical and numerical methods. Additionally, the associated phase portraits are provided for visualization of the results of the conducted analysis.

Phenomena like the multiplicative Allee effect and group defense significantly impact the system behavior and dynamics. This impact has been analyzed by studying the change in stable equilibrium point E_1^* as these parameters are varied. It is worth noting that multiplicative Allee effect parameters have no direct impact on the abscissa x_1^*, while the ordinate y_1^* is a decreasing function of m. Ecologically, it can be inferred that corresponding to the stable equilibrium point E_1^*, the prey population remains unaffected but the predator population decreases as the parameters m increase. The parameter can be increased up to the point where the condition $K + mK + \beta y_1^* e^{-\beta x_1^*} < 2Kx_1^*$ remains true. So, we have a threshold value for m, beyond which E_1^* will lose its stability and the system will either move towards a predator-free equilibrium point or collapse, contingent on the initial value of populations. Now, with regard to the group defense parameter β, it is noted that y_1^* is a decreasing function of β. This implies that the predator population corresponding to the stable equilibrium point E_1^* increases, as the group defense parameter is increased. The value that parameter β takes should be picked with great consideration as it needs to satisfy two conditions, $b > e\beta d$ and $K + mK + \beta y_1^* e^{-\beta x_1^*} < 2Kx_1^*$, simultaneously. The coexistence of both species is significantly influenced by the group defense parameter. As β exceeds the threshold value, the system will collapse or result in the persistence of only the prey species, depending on the initial populations.

This article sheds light on the development and analysis of a predator–prey model that integrates group defense mechanisms and the multiplicative Allee effect in prey. By examining how these factors influence population stability, predator–prey coexistence, and critical thresholds for extinction, a deeper understanding of the dynamic complexities inherent in the ecological system has been provided. Also, the initial population that the system commences with is a crucial factor in shaping the long-term behavior of the system.

Author Contributions: Conceptualization: M.K.S. and A.S.; methodology: M.K.S., A.S. and L.M.S.-R.; formal analysis: M.K.S. and A.S.; investigation: M.K.S., A.S. and L.M.S.-R.; writing—review and editing: M.K.S., A.S. and L.M.S.-R.; visualization: M.K.S. and A.S.; supervision: M.K.S. and L.M.S.-R. All authors have read and agreed to the published version of the manuscript.

Funding: This research received no external funding.

Data Availability Statement: Data are contained within the article.

Acknowledgments: The author Arushi Sharma expresses gratitude to Banasthali Vidyapith for providing the opportunity and inspiration to compose this research paper.

Conflicts of Interest: The authors declare no conflicts of interest.

References

1. Lotka, A.J. *Elements of Physical Biology*; Williams & Wilkins: Baltimore, MD, USA, 1925.
2. Volterra, V. Fluctuations in the abundance of a species considered mathematically. *Nature* **1926**, *118*, 558–560. [CrossRef]
3. Mandal, S.; Al Basir, F.; Ray, S. Additive Allee effect of top predator in a mathematical model of three species fod chain. *Energy Ecol. Environ.* **2021**, *6*, 451–461. [CrossRef]
4. Shang, Z.; Qiao, Y. Bifurcation analysis of a Leslie-type predator–prey system with simplified Holling type IV functional response and strong Allee effect on prey. *Nonlinear Anal. Real World Appl.* **2022**, *64*, 103453. [CrossRef]
5. Singh, M.K.; Poonam, P. Stability and bifurcation analysis of a harvested predator-prey model with toxicity and strong Allee effect. In Proceedings of the AIP Conference Proceedings, Jamshedpur, India, 21–22 December 2020; AIP Publishing: College Park, MD, USA, 2022; Volume 2435.

6. Jiao, X.; Li, X.; Yang, Y. Dynamics and bifurcations of a Filippov Leslie-Gower predator-prey model with group defense and time delay. *Chaos Solitons Fractals* **2022**, *162*, 112436. [CrossRef]
7. Shivam; Singh, T.; Kumar, M. Spatiotemporal dynamical analysis of a predator–prey system with fear and group defense in prey. *J. Biol. Syst.* **2022**, *30*, 387–422. [CrossRef]
8. Singh, M.K.; Sharma, A. Bifurcation analysis of a predator–prey model incorporating nonlinear harvesting and group defense. *Int. J. Biomath.* **2024**, *48*, 2450130. [CrossRef]
9. Wolkowicz, G.S.K. Bifurcation analysis of a predator-prey system involving group defence. *Siam J. Appl. Math.* **1988**, *48*, 592–606. [CrossRef]
10. Freedman, H.I.; Wolkowicz, G.S.K. Predator-prey systems with group defence: the paradox of enrichment revisited. *Bull. Math. Biol.* **1986**, *48*, 493–508. [CrossRef] [PubMed]
11. Freedman, H.I.; Ruan, S. Hopf bifurcation in three-species food chain models with group defense. *Math. Biosci.* **1992**, *111*, 73–87. [CrossRef] [PubMed]
12. Rothe, F.; Shafer, D.S. Multiple bifurcation in a predator–prey system with nonmonotonic predator response. *Proc. R. Soc. Edinb. Sect. Math.* **1992**, *120*, 313–347. [CrossRef]
13. Sasmal, S.K.; Takeuchi, Y. Dynamics of a predator-prey system with fear and group defense. *J. Math. Anal. Appl.* **2020**, *481*, 123471. [CrossRef]
14. Das, S.; Chattopadhyay, J.; Mahato, S.K.; Mahato, P. Extinction and persistence of a harvested prey–predator model incorporating group defence and disease in prey: Special emphasis on stochastic environment. *J. Biol. Syst.* **2022**, *30*, 423–457. [CrossRef]
15. Pratama, R.A.; Loupatty, M.; Hariyanto, H.; Caesarendra, W.; Rahmaniar, W. Fear and Group Defense Effect of a Holling Type IV Predator-Prey System Intraspecific Competition. *Emerg. Sci. J.* **2023**, *7*, 385–395. [CrossRef]
16. Pal, S.; Karmakar, S.; Pal, S.; Pal, N.; Misra, A.; Chattopadhyay, J. Impact of Fear and Group Defense on the Dynamics of a Predator–Prey System. *Int. J. Bifurc. Chaos* **2024**, *34*, 2450019. [CrossRef]
17. Souna, F.; Lakmeche, A.; Djilali, S. The effect of the defensive strategy taken by the prey on predator–prey interaction. *J. Appl. Math. Comput.* **2020**, *64*, 665–690. [CrossRef]
18. Kaushik, R.; Banerjee, S. Predator–prey system: Bachelor Herding of the prey imposes ecological constraints on predation. *Int. J. Bifurc. Chaos* **2021**, *31*, 2150211. [CrossRef]
19. Tang, B. Dynamics for a fractional-order predator-prey model with group defense. *Sci. Rep.* **2020**, *10*, 4906. [CrossRef] [PubMed]
20. Al-Momen, S.; Naji, R. The dynamics of sokol-howell prey-predator model involving strong Allee effect. *Iraqi J. Sci.* **2021**, *62*, 3114–3127. [CrossRef]
21. Kumar, U.; Mandal, P.S. Role of Allee effect on prey–predator model with component Allee effect for predator reproduction. *Math. Comput. Simul.* **2022**, *193*, 623–665. [CrossRef]
22. Rahmi, E.; Darti, I.; Suryanto, A.; Trisilowati. A modified Leslie–Gower model incorporating Beddington–DeAngelis functional response, double Allee effect and memory effect. *Fractal Fract.* **2021**, *5*, 84. [CrossRef]
23. Yin, W.; Li, Z.; Chen, F.; He, M. Modeling Allee Effect in the Leslie-Gower Predator–Prey System Incorporating a Prey Refuge. *Int. J. Bifurc. Chaos* **2022**, *32*, 2250086. [CrossRef]
24. Cruz, R.L. Stability of a Leslie-Gower type predator-prey model with a strong Allee effect with delay. *Sel. Mat.* **2022**, *9*, 24–33. [CrossRef]
25. Sen, D.; Ghorai, S.; Banerjee, M.; Morozov, A. Bifurcation analysis of the predator–prey model with the Allee effect in the predator. *J. Math. Biol.* **2022**, *84*, 7. [CrossRef] [PubMed]
26. Shang, Z.; Qiao, Y. Multiple bifurcations in a predator–prey system of modified Holling and Leslie type with double Allee effect and nonlinear harvesting. *Math. Comput. Simul.* **2023**, *205*, 745–764. [CrossRef]
27. Singh, M.K.; Sharma, A.; Sánchez-Ruiz, L.M. Dynamical Complexity of Modified Leslie–Gower Predator–Prey Model Incorporating Double Allee Effect and Fear Effect. *Symmetry* **2024**, *16*, 1552. [CrossRef]
28. Xiao, D.; Ruan, S. Codimension two bifurcations in a predator–prey system with group defense. *Int. J. Bifurc. Chaos* **2001**, *11*, 2123–2131. [CrossRef]
29. González-Olivares, E.; González-Yañez, B.; Mena-Lorca, J.; Flores, J.D. Uniqueness of limit cycles and multiple attractors in a Gause-typepredator-prey model with nonmonotonic functional response and Allee effecton prey. *Math. Biosci. Eng.* **2013**, *10*, 345–367.
30. Perko, L. *Differential Equations and Dynamical Systems*; Springer Science & Business Media: New York, NY, USA, 2013; Volume 7.

Disclaimer/Publisher's Note: The statements, opinions and data contained in all publications are solely those of the individual author(s) and contributor(s) and not of MDPI and/or the editor(s). MDPI and/or the editor(s) disclaim responsibility for any injury to people or property resulting from any ideas, methods, instructions or products referred to in the content.